Neuron, *Volume 73*

Supplemental Information

Gamma Oscillations Are Generated Locally in an Attention-Related Midbrain Network

C. Alex Goddard, Devarajan Sridharan, John R. Huguenard, and Eric I. Knudsen

Supplemental Experimental Procedures

LFP Preprocessing

LFP processing was performed using Matlab (2007a, The MathWorks, Natick, MA, USA). Line noise (60 Hz) and its second harmonic (120 Hz) were removed from the recording using the *rmlinesc* function, available from the Chronux toolbox (http://www.chronux.org). To obtain the LFP, the raw recordings were lowpass filtered at 200 Hz, and downsampled to 1kHz using the *resample* function in Matlab. Filters were designed in Matlab using the *buttord, butter, and filtfilt* functions to make zero-phase Butterworth filters with 0.1dB attenuation in the passband, and at least 3dB attenuation in the stop band.

Computing the Duration and Power of Oscillations in the OT

We define t_0 = time of electrical stimulation, and δ = duration of an episode. We computed the duration of gamma periodicity in the evoked response with the following algorithm: For every trial, the evoked response was examined in a response period extending from t_0+50 to t_0+2500 ms. The first 50 ms of the evoked response was excluded from the analysis to avoid contamination by the stimulation artifact. The signal was bandpass filtered in the low gamma range (25-50 Hz) with a fourth-order Butterworth filter. A pre-stimulation baseline period was defined for a time-window from t_0-375 to t_0-25 ms. To create a null distribution of gamma power at baseline, root-mean-squared (rms) values of the baseline signal were computed in non-overlapping 50 ms bins and were pooled across trials for each site. For each trial, we computed the rms value of the response in overlapping, sliding windows of 50 ms duration each, sliding in 1 ms steps. The duration (δ) was defined as the point when rms values in more than 40 out of 50 (80%) successive windows fell below the 99th percentile of the null distribution. For examples of analysis output, see Supp. Figure S1G. We also computed δ by non-parametric statistical comparison of response power in non-overlapping 50ms windows to the null distribution, and obtained qualitatively similar results albeit at a lower temporal resolution. For plots of drug treatments, durations for each site and condition were normalized to their respective values in the control condition.

The gamma power (in dB) in the evoked response was obtained with the following equation: $P=20*\log_{10}(R_s/R_b)$, where R_s = rms value from t_0+50 ms to $t_0+\delta$ ms, and R_b is the rms of the baseline; all signals were gamma-band filtered. This approach permitted the decoupling of the estimation of response duration from the estimation of spectral power of the oscillations, which was particularly important for manipulations that affected the duration without affecting the magnitude of the evoked oscillation (Figure 3D, S2F). One exception to this approach was in transected slices treated with APV (Figure 7, S7), in which the duration of activity with APV was too brief to be reliably estimated by the procedure described previously. Therefore, gamma power was measured from t_0+50 ms to t_0+100 ms. For plots of bath-applied drug treatment, gamma power for each site and condition was normalized to its value in the control condition.

We used a similar procedure for estimating the duration and power of the high frequency response (Supp. Fig S2B, E). The chief difference was that durations were estimated from raw traces that were downsampled to 3kHz, and high-pass filtered at 500Hz to yield only the high-frequency (spiking) activity.

LFP Spectrograms

Spectrograms were computed with the multitaper approach using the Chronux software package (http://www.chronux.org). Spectrograms of the induced response were computed after subtracting the mean evoked response across stimulus repetitions for each site. Spectrograms were computed in a moving window of 300 ms (5 ms steps) with 3 tapers permitting a spectral resolution of ±6.7Hz (Supp. Figure S2, S6, S7). The only exceptions were Supp. Figure S2C and S2F. For Supp. Figure S2C (bath application of pentobarbital), a longer moving window (500 ms) was used to permit greater spectral resolution (±4Hz) so as to better highlight the changes in frequency of the induced oscillation. For Supp. Figure 2F (bath application of DHβE + atropine), a shorter moving window (150 ms) was used to permit greater temporal resolution so as to better demonstrate the differences in duration of the induced oscillation. Spectrograms averaged over 5-20 stimulus repetitions for each site and condition (Supp. Figure S2, S6, S7). The power in each frequency was normalized to the spectral power at the same frequency computed over 300 ms of baseline, and reported in units of dB relative to baseline. The first 10 ms following each stimulation was not analyzed to avoid contamination from the stimulus artifact (black bars in the same figures).

Computing the Duration of Spontaneous Events in Ipc (Figure S4)

Two similar analyses were performed on events filtered between 25-50 Hz for gamma power or above 250 Hz for high frequency spiking. The protocols for gamma analyses will be presented below (with the altered parameters for high frequency analyses in parentheses).

Traces were downsampled to 1kHz (10kHz), and filtered between 25-50 Hz (> 250 Hz). The RMS was calculated over a sliding window of 50 ms (10 ms), with a 1 ms (0.1 ms) interval between each window. A baseline window of 1 second was selected by visual inspection; baseline windows were chosen to have no large excursions. A mean (x) and standard deviation (σ) for the RMS were determined using this baseline window. The RMS-transformed waveform was then broken up into an array of 25 ms (5 ms), non-overlapping bins, and a threshold of $x + 3*\sigma$ was applied to detect all bins that had potential events. The duration of the event was determined as the beginning of the first suprathreshold bin to the beginning of the last suprathreshold bin and, thus, was limited to a time resolution of 25 ms (5 ms). Positive events in the first bin of the trace or that were contiguous with the last bin of the trace were eliminated. Events lasting longer than 150 ms (100 ms) were deemed to be persistent.

Spectra of Membrane Potentials and Spikes (Ipc Sharp Recordings, Fig 5)

For sharp electrode recordings in the Ipc, we analyzed sub-threshold potentials in epochs during which the neuron was receiving EPSPs, but fired very few spikes. This trace was downsampled to 1kHz, lowpass filtered at 200Hz, and its spectrum was estimated with the multitaper approach for continuous signals. To compute the spectrum of the bursts, epochs during which the neuron fired robustly were used. We filtered the raw recordings between 0.5-3.5 kHz, extracted the spike-times using a threshold of 4x the standard deviation of the membrane voltage. These spike times were analyzed with a multitaper spectral estimation algorithm for point processes (Chronux toolbox, http://www.chronux.org).

Analysis of Coherence between the Extracellular LFP and Intracellular Currents (Figure 6, S6)

We analyzed the timing of intracellular synaptic currents relative to the extracellular LFP with the multitaper method (Womelsdorf et al., 2007; Pesaran et al., 2002). Synaptic currents (EPSCs and IPSCs) exhibited rapid onsets followed by a decay with slower kinetics. Because we were less interested in the rise and decay kinetics of the PSCs, and specifically interested in their timing relative to the extracellular LFP phase, we developed a procedure for detecting PSC onset times. We created a differentiating filter (difference-of-

Gaussians filter for edge detection) with a duration suited to detecting the onsets of excitatory and inhibitory currents in the time domain. PSC onset times were reliably identified by this procedure, as verified by visual inspection. We then performed a coherence analysis of the PSC times with the induced broadband (5-200Hz) LFP signal using the multitaper approach (Chronux toolbox, Bokil et al., 2010). One second of the signal (post-stimulation) was analyzed with a time-bandwidth product of 20, employing 39 tapers, which permitted a spectral concentration over ±20Hz. The phase relationship between the tapered LFP and the PSCs was quantified as the angle of the complex-valued cross-spectrum (Womelsdorf et al., 2007) in the 25-50Hz band. The distribution of temporal delays between the EPSC and IPSC onsets across sites was computed based on the difference between the EPSC-LFP and IPSC-LFP phase for each site, and subjected to a Wilcoxon signed rank test against the null hypothesis of zero difference (corresponding to no delay between EPSCs and IPSCs). Analysis with the peak times (instead of onset times) of the intracellular currents resulted in similar timing relationships of the EPSC and IPSC peaks to LFP phase, albeit lagged by an amount equivalent to the PSC rise time (~1 ms).

We calculated the LFP (25-50Hz) trough-triggered average of intracellularly recorded EPSCs and IPSCs using a procedure employed in previous studies (Fisahn et al., 1998; Hasenstaub et al., 2005). Briefly, we filtered the extracellular LFP (1s post-stimulation) for a 25-50Hz band, and identified the troughs of this signal using a second-derivative test. We then assembled snippets of E/IPSC recordings in a ±25 ms window around each trough for each LFP cycle, and averaged these PSC waveforms across > 7000 cycles. For ease of comparison with IPSCs, EPSC waveforms were inverted from their conventional representation prior to this procedure, such that the peak of the EPSC represents maximum inward current (Figure 6F). We confirmed the results with a second analysis, in which we interchanged the triggering and averaged signals: we averaged snippets of the filtered LFP waveform triggered off the PSC event times (onsets). LFP waveforms, filtered in the 25-50 Hz band, were averaged across events for each site, and then averaged across sites for each event type (EPSCs or IPSCs) to identify systematic differences in the phase of the gamma cycle, across sites, at the onset of each event type (Supple. Figure S6).

Analysis of Bursts and LFP in sOT Recordings (Figure S3)

We first separated each trace into a high-pass (> 200 Hz) filtered version to find bursts, and a low-pass (< 200 Hz) filtered version to find the LFP, using the *filtfilt* function in Matlab. Bursts were detected by finding clusters of peaks (above a visually validated threshold) in the high-pass signal. A burst was defined as lasting over 2 ms. The start and end time of the burst, as well as the RMS value during each burst period was calculated. An example output of the detection bursts is shown in Figure S3B (green lines above trace).

To assess the magnitude of the burst-associated LFP, the low-pass signal in a time window of 20 ms either preceding or following the burst start time were analyzed. The peak-to-peak amplitude of the LFP was found within these time windows.

The burst amplitude and LFP amplitude pairs were compared using the *robustfit* function in Matlab, which produced the slope and intercept for a line of best fit and an associated p-value. The correlation coefficient was calculated using *corrcoef* function.

For plotting, max values of the burst and LFP were normalized to 1 for each site.

Labeling and Immunofluorescence

In vitro slices were prepared and placed into a static interface chamber. 1% biocytin was dissolved in ACSF and pressure injected into the Ipc. Slices were incubated for >4 hours. Slices were fixed in 4% paraformaldehyde overnight and sunk in 30% sucrose and resectioned to 50 μm sections. Sections were

incubated in phosphate buffered saline + 0.1% Triton X-100 (PBST) with 1/100 Neutravidin Oregon Green 488 (Invitrogen) and 1/100 Neurotrace 530/615 fluorescent Nissl stain (Invitrogen) for 1 hour, then washed and coverslipped.

For immunodetection of parvalbumin and CamKII, sections were placed in 5% normal goat serum in PBST ("block solution") for 1 hour. Primary antibodies were diluted in the block solution: mouse anti-CaMKII (Abcam, ab22609): 1/500; mouse anti-parvalbumin (Sigma, P3088): 1/2000, for 2 nights at 4º C. Secondary antibodies were added at 1/300 to the block solution for 2 hours. Images were acquired using a Zeiss LSM 510 Confocal microscope with a 63x Plan Neofluar objective. A montage of images was acquired with the MultiTime macro. Z-stacks were compressed to a maximum projection and stitched using Fiji image analysis software.

Supplemental References

Bokil, H., Andrews, P., Kulkarni, J. E., Mehta, S., and Mitra, P. P. (2010). Chronux: a platform for analyzing neural signals. Journal of Neuroscience Methods *192*, 146–151.

Fisahn, A., Pike, F. G., Buhl, E. H., and Paulsen, O. (1998). Cholinergic induction of network oscillations at 40 Hz in the hippocampus in vitro. Nature *394*, 186–189.

Hasenstaub, A., Shu, Y., Haider, B., Kraushaar, U., Duque, A., and McCormick, D. A. (2005). Inhibitory postsynaptic potentials carry synchronized frequency information in active cortical networks. Neuron *47*, 423–435.

Pesaran, B., Pezaris, J. S., Sahani, M., Mitra, P. P., and Andersen, R. A. (2002). Temporal structure in neuronal activity during working memory in macaque parietal cortex. Nat Neurosci *5*, 805–811.

Womelsdorf, T., Schoffelen, J.-M., Oostenveld, R., Singer, W., Desimone, R., Engel, A. K., and Fries, P. (2007). Modulation of neuronal interactions through neuronal synchronization. Science *316*, 1609–1612.

Figure S1

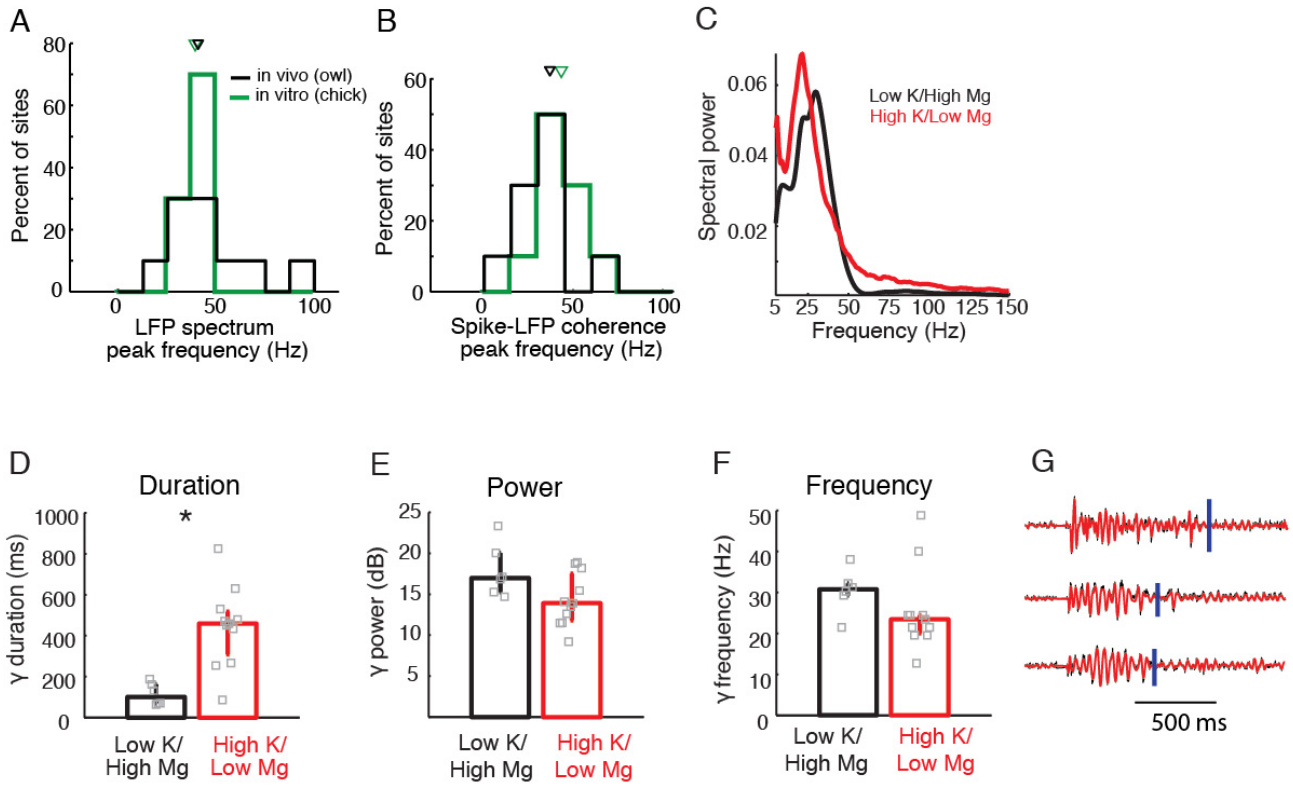

Figure S1. Comparison of Gamma Oscillations sOT In Vivo and In Vitro, Related to Figure 1

(A) Distribution of peak frequencies of the induced LFP response recorded in the sOT from *in vitro* (green, n=10 slices) and *in vivo* (black, n=10 sites) preparations (same recordings as in Figure 1E, main text). Inverted triangles: Population medians.

(B) Distribution of peak frequencies of the spike-LFP coherence. Other conventions same as in (A).

(C) Average spectra for oscillations recorded in differing levels of K^+ and Mg^{++}. Gamma power is equivalent in both conditions. Low K^+ condition= 2.5 mM K^+, 2 mM Mg^{++} (n=6); High K^+ condition= 3.5 mM K^+, 1 mM Mg^{++} (n=11).

(D) Duration of persistent gamma oscillations was reduced by reducing K^+ and raising Mg^{++} concentrations (Low K^+: 101 ms, High K^+: 459 ms**,** p=0.01, Mann-Whitney U test). Squares indicate the median value for individual sites, based on responses to 10-40 stimulus repetitions.

(E) Gamma power was not altered by changing cation concentrations (Low K^+: 17 dB, High K^+: 14 dB, p=0.56, Mann-Whitney U test, Bonferroni corrected for multiple comparisons). Conventions as in (D).

(F) Gamma duration was not altered by changing cation concentrations (Low K^+: 31 Hz, High K^+: 23.5 Hz**,** p=1.0, Mann-Whitney U test, Bonferroni corrected for multiple comparisons). Conventions as in (D).

(G) Example output of duration detection analysis. LFP traces (red) filtered in the gamma range (25-50 Hz). Estimates of duration of gamma periodicity in the evoked response (Experimental Procedures) are indicated by the vertical bar (blue).

Figure S2

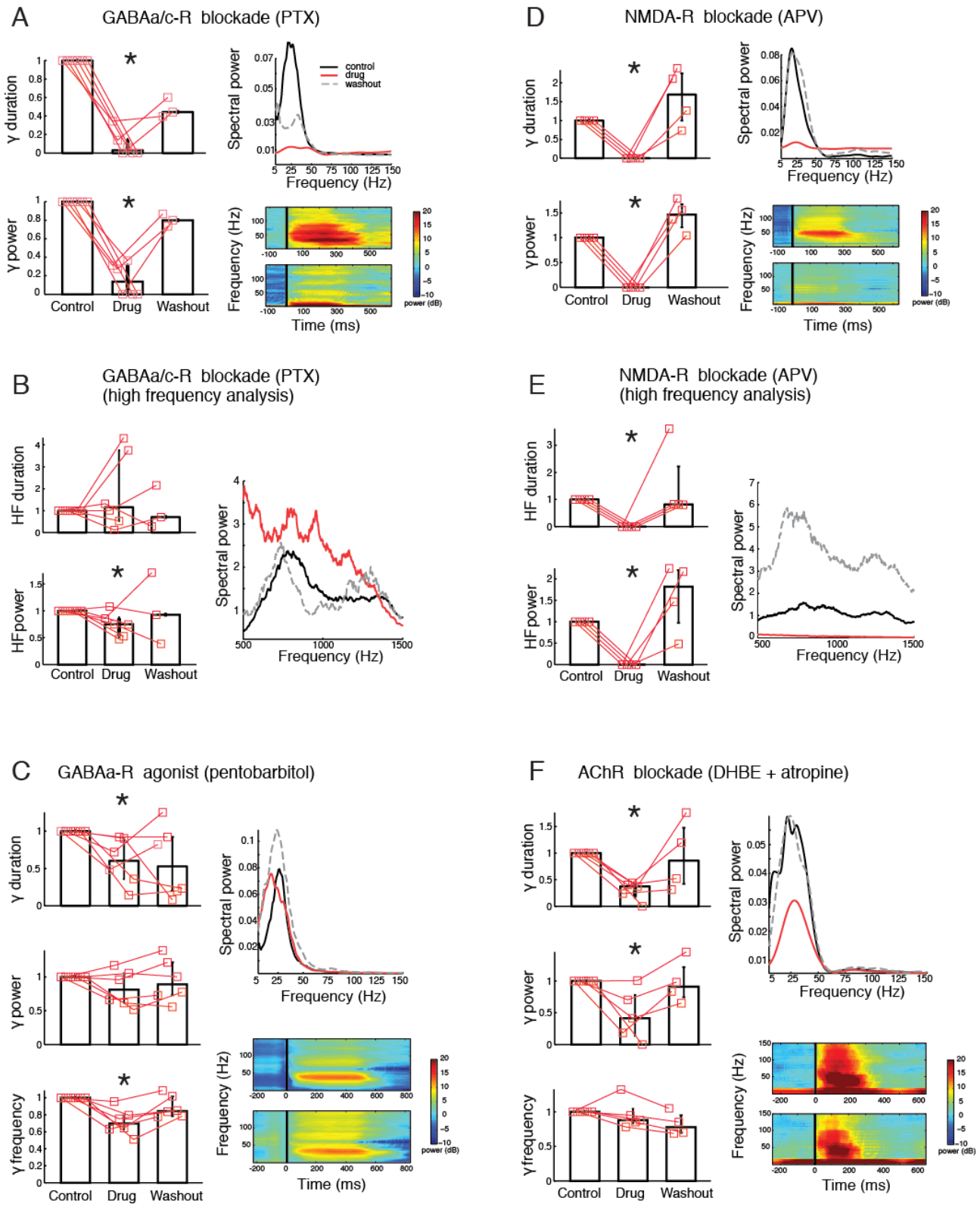
A
GABAa/c-R blockade (PTX)
γ duration
γ power
Control
Drug
Washout
Spectral power
control
drug
washout
Frequency (Hz)
Frequency (Hz)
Time (ms)
power (dB)
D
NMDA-R blockade (APV)
B
GABAa/c-R blockade (PTX)
(high frequency analysis)
HF duration
HF power
E
NMDA-R blockade (APV)
(high frequency analysis)
C
GABAa-R agonist (pentobarbitol)
γ frequency
F
AChR blockade (DHBE + atropine)

Figure S2. Multiple Neurotransmitter Systems Contribute to Gamma Oscillations in the OT, Related to Figure 3

Format for all figures:

(Left) Durations and power of evoked gamma oscillations under various, bath applied drug treatments. Bars represent medians (across sites) relative to control, and error bars are 25th and 75th percentiles. Red squares: median value for individual sites, based on responses to 10-40 stimulus repetitions.

(Right, top) Average spectra for control (black), drug (red) and washout (grey). (*Right, middle-bottom*) Spectrograms of the induced response from a representative site in the sOT at baseline/control (*middle*), and after drug treatment (*bottom*). For all spectrograms, t=0 ms represents the onset of stimulation. Black bar: 10ms following stimulation excluded due to stimulation artifact. Colorbar: Power in dB relative to baseline. All p-values compare drug condition with control or washout and are based on a Friedman test (non-parametric version of the repeated measures ANOVA) with Bonferroni correction for multiple comparisons. Gamma frequencies were not estimated for the PTX and APV drug conditions (A and C) due to insufficient gamma power in the evoked responses under drug treatment.

A) **PTX (10 μM)**:
Gamma duration:
Drug/Control = 2.9% ($p<0.001$, n=6);
Washout/Control = 44.2% ($p=0.012$, n=3/6).
Gamma power:
Drug/Control = 13.7% ($p<0.001$, n=6);
Washout/Control = 80.0% ($p=0.001$, n=3/6).

B) PTX high frequencies (HF, >500Hz):
HF duration:
Drug/Control = 116.1% ($p>0.9$, n=6);
Washout/Control = 70.8% ($p>0.9$, n=3/6).
HF power:
Drug/Control = 74.9% ($p=0.032$, n=6);
Washout/Control = 92.8% ($p>0.9$, n=3/6).

C) Pentobarbital (10 μM):
Gamma duration:
Drug/Control = 60.15% ($p<0.001$, n=6);
Washout/Control = 91.9% ($p=0.015$, n=3/6).
Gamma power:
Drug/Control = 81.2% ($p=0.89$, n=6);
Washout/Control = 89.0% ($p=0.76$, n=6/6)
Gamma frequency:
Drug/Control = 69.8% ($p<0.001$, n=6);
Washout/Control = 84.4% ($p=0.08$, corrected, $p=0.003$, uncorrected, n=6/6)

D) APV (25 μM):
Gamma duration:
Drug/Control = 0.0% ($p<0.001$, n=4);
Washout/Control = 168.6% ($p<0.001$, n=4/4).
Gamma power:
Drug/Control = 0.0% ($p<0.001$, n=4);
Washout/Control = 146.6% ($p<0.001$, n=4/4)

E) **APV high frequencies (HF, >500Hz):**
HF duration:
Drug/Control = 0.0% ($p<0.001$, n=4);
Washout/Control = 137.3% ($p<0.001$, n=4/4).
HF power:
Drug/Control = 0.0% ($p<0.001$, n=4);
Washout/Control = 110.6% ($p<0.001$, n=4/4).

F) DHBE (40 μM)+ Atropine (5 μM):
Gamma duration:
Drug/Control = 44.4 % ($p<0.001$, n=5);
Washout/Control = 86.3% ($p<0.001$, n=4/5).
Gamma power:
Drug/Control = 61.2% ($p<0.001$, n=5);
Washout/Control = 90.4% ($p=0.005$, n=4/5)
Gamma frequency:
Drug/Control = 87.9% ($p>0.9$, n=5);
Washout/Control = 77.8% ($p=0.004$, n=4/5

Figure S3

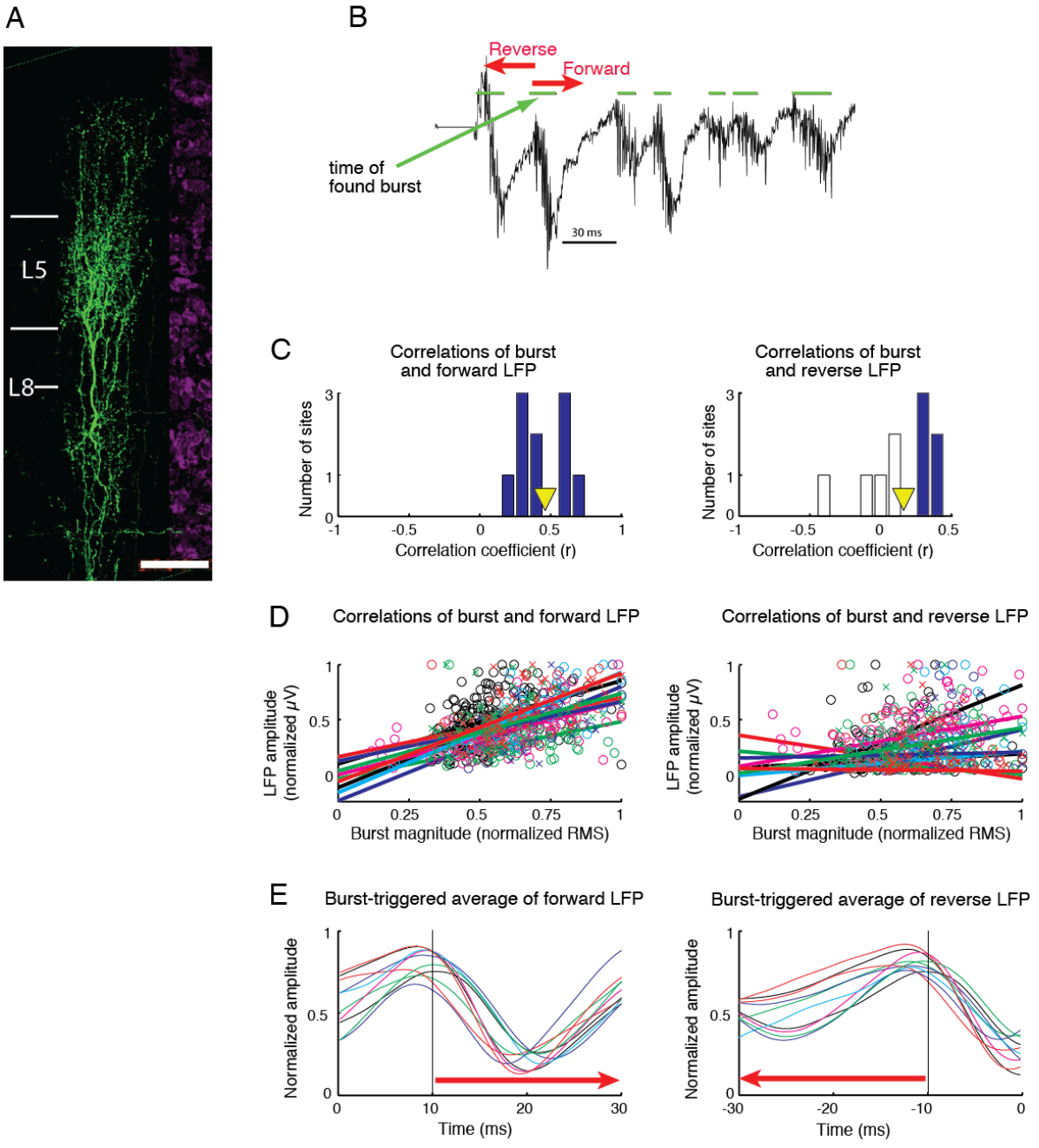
A
L5
L8
B
Reverse
Forward
time of
found burst
30 ms
C
Correlations of burst
and forward LFP
Number of sites
Correlation coefficient (r)
Correlations of burst
and reverse LFP
Number of sites
Correlation coefficient (r)
D
Correlations of burst and forward LFP
LFP amplitude
(normalized μV)
Burst magnitude (normalized RMS)
Correlations of burst and reverse LFP
LFP amplitude
(normalized μV)
Burst magnitude (normalized RMS)
E
Burst-triggered average of forward LFP
Normalized amplitude
Time (ms)
Burst-triggered average of reverse LFP
Normalized amplitude
Time (ms)

Figure S3. Relationship of High-Frequency Ipc Axon Bursts and LFP in sOT, Related to Figure 4

(A) Image of Ipc axon (green) labeled in an *in vitro* slice showing extensive ramifications in sOT, particularly in layer 5. Scale bar, lower right = 50 μm.

(B) Analysis of example trace from the sOT. Green bars above the trace indicate the time and duration of a high-frequency Ipc burst detected by the analysis program. Red arrows indicate the 20 ms portion of the LFP (2-200 Hz) analyzed preceding ('reverse') or following ('forward') the beginning of a burst.

(C) Correlation coefficients comparing the RMS amplitude of the burst and the peak-to-peak amplitude of the LFP are strong for forward LFP (*left*), but weak for reverse LFP (*right*) at 10 sites. Blue bars represent significant correlation ($p < 0.05$), while white bars represent correlations with $p > 0.05$. Yellow triangle indicates average coefficient (r). Forward correlation, average $r = 0.48$ was greater than zero, $p < 0.05$, Wilcoxon signed rank test. Reverse correlation, average $r = 0.20$, was not different from zero, $p > 0.05$, Wilcoxon signed rank test.

(D) Plots of burst magnitude vs LFP amplitude, and lines of best fit for 10 sites. Average slope for forward LFP (*left*, 0.79±0.23) was significantly higher than for the reverse LFP (*right,* 0.30±0.35). Values of burst RMS and LFP amplitude are normalized for each site. Each x or o represent a single burst-LFP event, and each color represents a different site.

(E) Burst-triggered averages of the LFP in the forward (*left*) and reverse (*right*) directions. Forward LFP reliably shows a larger amplitude and more periodic signal than the reverse LFP. Red arrows depict the window for LFP amplitude analysis used for correlations in (B) and (C). Each color represents a different site.

Figure S4

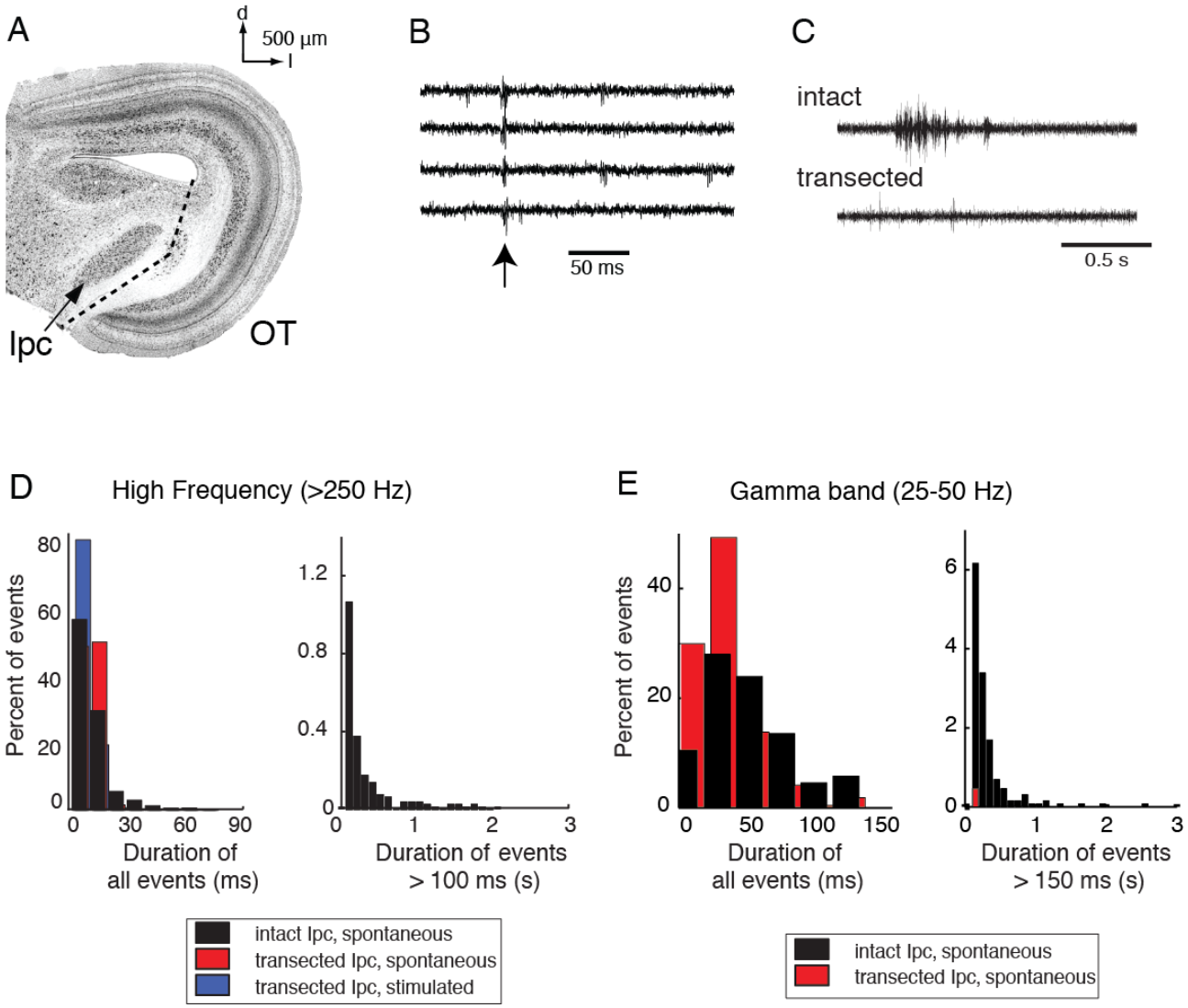
A
d
500 µm
l
lpc
OT
B
50 ms
C
intact
transected
0.5 s
D
High Frequency (>250 Hz)
Percent of events
Duration of all events (ms)
Duration of events > 100 ms (s)
intact lpc, spontaneous
transected lpc, spontaneous
transected lpc, stimulated
E
Gamma band (25-50 Hz)
Percent of events
Duration of all events (ms)
Duration of events > 150 ms (s)
intact lpc, spontaneous
transected lpc, spontaneous

Figure S4. Ipc Does Not Generate Persistent Oscillations without OT Input, Related to Figure 5

(A) Schematic of transection of connections between OT and the Ipc in the midbrain slice. Image is the same as in Figure 1A.

(B) Non-persistent responses in the Ipc following electrical microstimulation of Ipc inputs in transected slices. Four sequential traces from the same Ipc site are shown. Time of stimulation denoted by the arrow.

(C) *(Upper traces)* Representative traces of spontaneous, persistent events recorded in the Ipc in intact *(top)* and transected *(bottom)* slices. Same traces as in Figure 5C, top.

(D) Distribution of the durations of spiking events recorded in the Ipc for the experiments described in B and C. Events were detected in 5 millisecond bins. (*Left*) In all conditions, a majority of the events were short duration (< 20 ms). The distributions of durations from intact and transected slices are significantly different (Mann-Whitney U-test, $p<0.001$)

condition	**25th percentile**	**median**	**75th percentile**
Intact, spontaneous N=6 slices, 7979 events	10 ms	10 ms	15 ms
Transected, spontaneous N=5 slices, 11679 events	10 ms	10 ms	10 ms
Transected, evoked N=7 slices, 1880 events	5 ms	5 ms	10 ms

(Right) Persistent events (lasting more than 100 ms, or 20 consecutive bins) were only observed in the Ipc when connections with the OT were intact (black bars). Median duration [25th, 75th percentiles] = 215 ms [130 ms, 422.5 ms]. In transected slices (red bars), only one site had a single, spontaneous, persistent response, lasting 240 ms; no persistent events were evoked.

(E) Distribution of the durations of events with gamma power recorded in the Ipc for the experiments described in C. Events were detected in 50 millisecond bins. (*Left*) In all conditions, a majority of the events were short duration (< 100 ms). The distributions of durations from intact and transected slices are significantly different (Mann-Whitney U-test, $p<0.001$)

condition	**25th percentile**	**median**	**75th percentile**
Intact, spontaneous N=6 slices, 1298 events	50 ms	50 ms	100 ms
Transected, spontaneous N=5 slices, 217 events	25 ms	25 ms	50 ms

(Right) Persistent events (lasting more than 150 ms, or 3 consecutive bins) were only observed in the Ipc when connections with the OT were intact (black bars). Median duration [25th, 75th percentiles] = 215 ms [130 ms, 422.5 ms]. In transected slices (red bars), only one site had a single persistent response, lasting 200 ms.

Figure S5

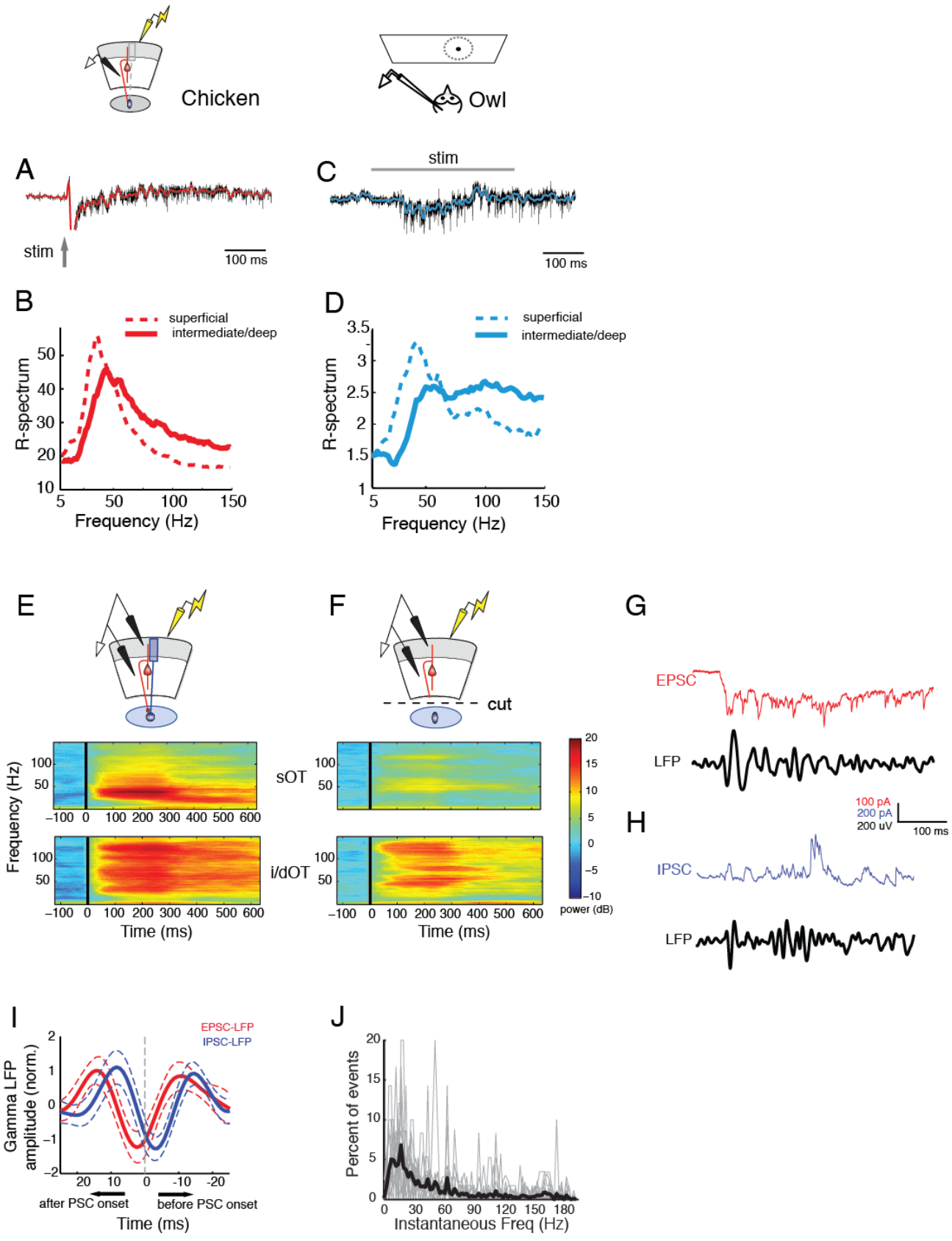
Chicken
Owl
A
stim
100 ms
C
stim
100 ms
B
superficial
intermediate/deep
R-spectrum
Frequency (Hz)
D
superficial
intermediate/deep
R-spectrum
Frequency (Hz)
E
Frequency (Hz)
sOT
i/dOT
Time (ms)
F
cut
Time (ms)
power (dB)
G
EPSC
LFP
H
100 pA
200 pA
200 uV
100 ms
IPSC
LFP
I
EPSC-LFP
IPSC-LFP
Gamma LFP amplitude (norm.)
after PSC onset
before PSC onset
Time (ms)
J
Percent of events
Instantaneous Freq (Hz)

Figure S5. Gamma Oscillations in the sOT and i/dOT Are Similar In Vivo and In Vitro and PSC-LFP Correlation, Related to Figure 6

(Top) Schematics indicating recordings from the i/dOT *in vitro* (left) and *in vivo* (right).

(A) Representative trace (black) of gamma oscillations from the i/dOT of the chick slice in response to a 0.1 ms stimulus delivered to the retinal afferents. Grey arrow: stimulus pulse. Red: 25-50Hz filtered LFP.

(B) Spectra showing sOT (dashed line) and broader i/dOT (solid line) gamma band power from an *in vitro* chick slice recording (spectra shown are averaged from n=10 slices).

(C) Representative trace (black) of gamma oscillations recorded from the i/dOT of an owl (*in vivo)* in response to a 350 ms visual stimulus. Grey bar above the trace indicates stimulus presentation. Blue: 25-50Hz filtered LFP.

(D) Spectra showing sOT (dashed line) and broader i/dOT (solid line) gamma band power from *in vivo* owl recordings (spectra shown are averaged from n=10 sites).

(E) Spectrograms of the induced LFP response recorded simultaneously with a rake electrode (Experimental Procedures) for a representative site in the sOT (top) and i/dOT (bottom). t=0 ms represents the onset of stimulation. Black bar: 10ms following stimulation excluded due to stimulation artifact. Colorbar: Power in dB relative to baseline.

(F) Spectrograms of the induced LFP response at the same site after surgical transection of the Ipc. Other conventions are as in panel (A).

(G) Example of simultaneously recorded EPSCs in an L10 neuron held at -65 mV (top) and the LFP nearby (bottom).

(H) Example of simultaneously recorded IPSCs in an L10 neuron held at 0 mV (top) and the LFP nearby (bottom).

(I) LFPs filtered in the 25-50Hz band were averaged within a ±25 ms window around each post-synaptic event, centered on the onsets of the EPSCs (red), or IPSCs (blue). Dashed vertical line: t=0 corresponding to PSC onset. Dashed lines: 95% confidence intervals across n=17 sites. For clarity of presentation the time axis has been inverted such that times to the right of t=0 precede (lead) PSC onsets, and times to the left of t=0 follow (lag) the PSC onset.

(J) L10 neuron spiking recorded extracellularly following retinal afferent stimulation in slices transected from the Ipc. Median firing rate of 32.5 Hz, 25^{th} percentile: 24.5 Hz, 75^{th} percentile: 39.5 Hz, n=16). Thin, gray lines represent spectra from individual cells, heavy black line represents average spectrum.

Figure S6

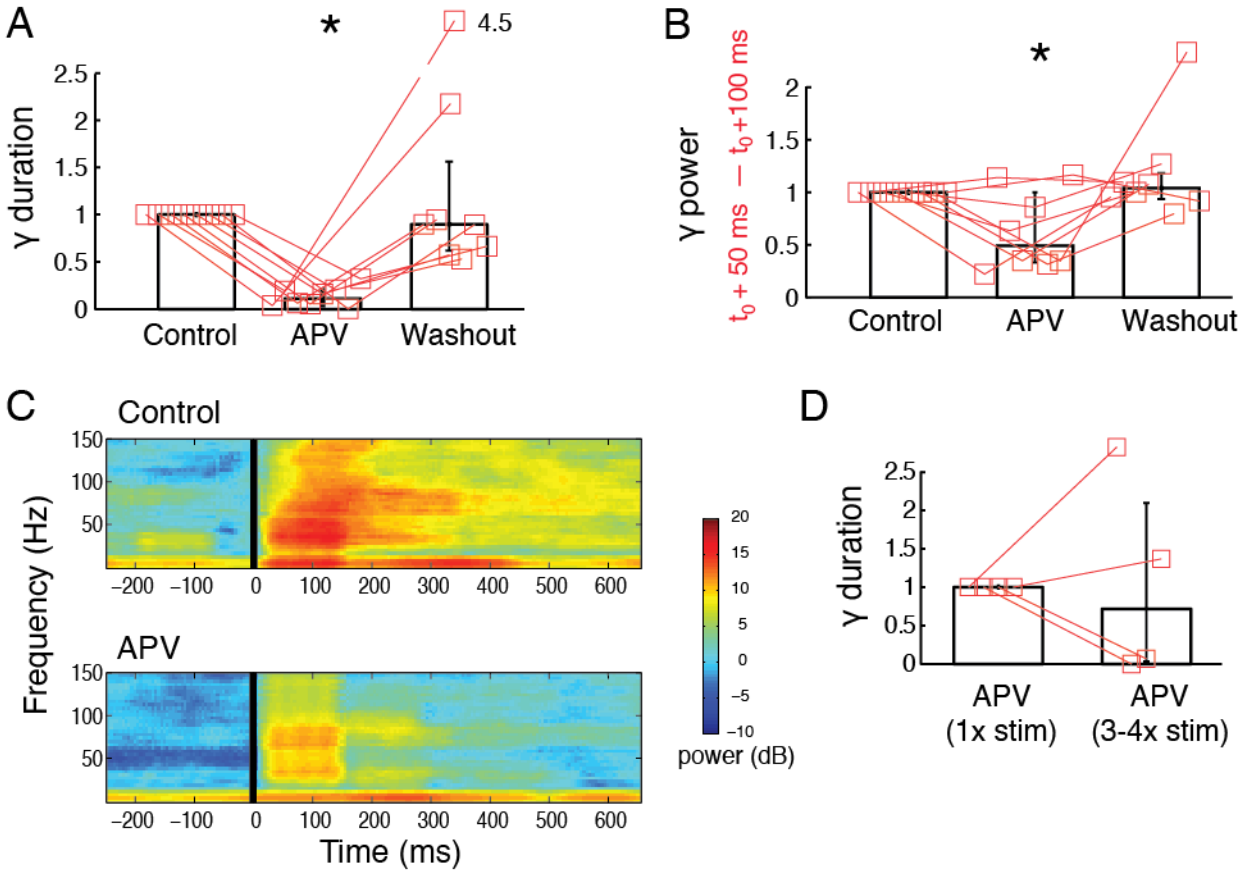

Supplemental Figure S6. APV eliminates persistence but not gamma power in transected i/dOT, Related to Figure 7

Conventions are the same as in Figure S2.

(A) Duration, relative to control, of induced gamma activity in the i/dOT after application of APV to a transected slice. Gamma duration: drug/control = 11.1% ($p<0.001$, n=8); washout/control = 89.6% ($p<0.001$, n=8/8).

(B) Same as in A, but for induced gamma power. Induced gamma power was computed for a time window extending from t_0+50 to t_0+100 ms, where t_0 is the time of stimulation. Gamma power: drug/control = 49.3% ($p<0.001$, n=8); washout/control = 103.9% ($p<0.001$, n=8/8).

(C) Spectrogram of gamma oscillations in control condition (top) and after applying APV (bottom). Other conventions are as in Supplemental Figure S6.

(D) Increasing the strength of retinal afferent stimulation by a factor of 3-4x does not increase the duration of induced gamma activity during APV application. Ratios are relative to 1x stim under APV: duration (3-4x stim)/duration (1x stim) = 71.8% ($p>0.9$, n=4).

Figure S7

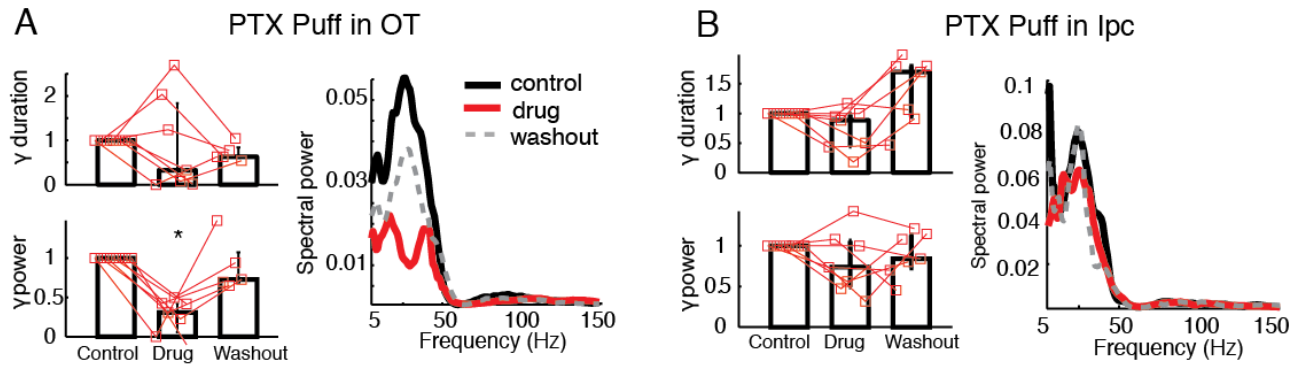

Figure S7. Focal Application of Picrotoxin to the OT and Ipc, Related to Figure 8
Conventions are the same as in Figure S2.

(A) Gamma durations and power following focal application of PTX to the *OT* (n=7). *(Top left)* Durations of gamma oscillations were not significantly affected (33% of control, p=0.9, Friedman test). *(Bottom left)* Gamma power was significantly reduced (31% of control, p<0.001, Friedman test) and showed significant recovery in 70% (n=5/7) of the sites.*(Right)* Average power spectra of gamma oscillations in the sOT before (black) and after (red) PTX puff in the OT. Grey: spectrum following washout.

(B) Gamma durations and power following focal application of PTX to the *Ipc* (n=7). *(Top left)* Durations of gamma oscillations were not significantly affected (88% of control, p=0.38, Friedman test). *(Bottom left)* Gamma power was significantly reduced (74% of control, p=0.55, Friedman test). *(Right)* Average power spectra of gamma oscillations in the sOT before (black) and after (red) PTX puff in the Ipc (n=7). Grey: spectrum following washout.